Quantum Interference Effects in Self-Assembled Asymmetric Disulfide Monolayers: Comparisons between Experiment and *ab Initio*/Monte Carlo Theories

Jun Cheng and Cary J. Miller*

Department of Chemistry and Biochemistry, University of Maryland at College Park, College Park, Maryland 20742

Received: September 6, 1996; In Final Form: December 4, 1996[⊗]

Electron transfer measurements between solution redox probes and a Au electrode coated with self-assembled monolayers of symmetric and asymmetric ω-hydroxyalkane disulfides are used to probe the quantum interference between hydrocarbon chains of different lengths. While *ab initio* theory predicts a measurable destructive interference effect between hydrocarbon chains differing in length by a single methylene unit, electron transfer rates for the ferricyanide and horse heart cytochrome *c* are more consistent with rates estimated in the absence of the interference effect. The discrepancy between theory and experiment is discussed in light of possible interchain electronic coupling and phase segregation within the monolayers and limitations of the theoretical models.

1. Introduction

Electron transfer reactions occurring over large distances play important roles in biological and technological systems. The rates of these electron transfers depend on the electronic coupling between the donor and acceptor states, which is a function of the intervening molecular material. The electronic coupling interactions between the donor and acceptor generally proceed through a large number of pathways which are describable as the interactions between particular orbitals on the intervening atoms. A notable feature of these electronic coupling pathways is that they are signed quantities which can sum constructively or destructively to give rise to the overall electronic coupling.[1] In building donor/acceptor systems for biomimetic, photovoltaic, or other technological uses, the quantum interference between electronic coupling pathways should be an important design consideration. The investigation of the interference between tunneling pathways has received relatively little attention, particularly in regard to its use in designing spacer geometries. Recently, Shephard and Paddon-Row have presented a parity rule for the design of rigid hydrocarbons with enhanced or diminished electronic coupling due to pathway interference.[2] While this previous work has focused on intramolecular interference effects, the principle should also be operative intermolecularly within spacers comprised of assemblages of molecules.

Studies using self-assembly of alkanethiols and disulfides on Au electrodes have shed considerable light on the structural dependence of the electronic coupling. These self-assembled monolayers function as electron-tunneling barriers forcing electron transfer reactions at such monolayer-coated electrodes to proceed *via* an extremely nonadiabatic electron transfer mechanism. The relative electronic coupling between different monolayers is obtained from a simple comparison of their heterogeneous electron transfer rates to pendant or freely diffusing redox probes.[3] A particular strength of these monolayer systems is that their internal structures can be controlled at the atom level simply by control of the structure of the amphiphile used to form the monolayer.[4] The relatively simple structure of these tunneling barriers facilitates comparisons with *ab initio* calculations. In these *ab initio* studies, it has been noted that the sign of the electronic coupling estimates changes between even and odd hydrocarbon chain lengths.[4,5] If one were to produce a mixed alkanethiolate monolayer having both even and odd chain lengths, the electronic coupling proceeding through nearby chains with different lengths would be predicted to interfere destructively, giving rise to lower electron transfer rates.

In this paper we probe the electronic coupling properties of monolayers formed by symmetric and asymmetric ω-hydroxyalkane disulfides. The monolayers formed by disulfides have been shown to be functionally identical to those formed with thiols.[6] An advantage of using disulfides for the production of monolayers containing different thiolate chains is that self-segregation of the different chains into separate domains can be minimized.[7] The experimentally determined electronic coupling through these asymmetric disulfide films is compared with simple *ab initio* estimates and more sophisticated Monte Carlo predictions.

2. Experimental Section

Syntheses: 11-Hydroxyundecyl 12′-Hydroxydodecyl 1,1′-Disulfide (C11−12) and 10-Hydroxydecyl 11′-Hydroxyundecyl 1,1′-Disulfide (C10−11). $HO(CH_2)_nOH$ (n = 10, 12) was converted to $I(CH_2)_nI$ (n = 10, 12) *via* reflux in 51% aqueous HI for 2 h. After flash chromatographic purification (silica gel, heptane), the diiodoalkane was treated with 1 equiv of thiourea, refluxed for 1 h in 95% ethanol, treated with a slight excess of NaOH under nitrogen for 20 min, and then neutralized with dilute HCl. The ethanol was removed under reduced pressure, and the product was extracted from the aqueous phase using $HCCl_3$. The crude $I(CH_2)_nSH$ (n = 10, 12) was purified by column chromatography (silica, heptane). To an equal molar solution of $I(CH_2)_nSH$ and $HO(CH_2)_{11}SH$ (prepared from $Br(CH_2)_{11}OH$) as described previously[8]) was added I_2 (10 mM in 95% ethanol) slowly while the solution was heated to 40 °C. Iodine was added until a persistent yellow-brown color was observed.[7b,9] The $I(CH_2)_nSS(CH_2)_{11}OH$ (n = 10, 12) was purified *via* column chromatography (silica, chloroform). This iodide was hydrolyzed to the diol *via* heating at 100 °C in a solution of 15% H_2O in HMPA.[10] The C11−10 and C11−12 were purified by column chromatography (silica, ethyl acetate: chloroform; 15:85, w/w). The purity of the asymmetric

* To whom correspondence should be addressed.

[⊗] Abstract published in *Advance ACS Abstracts,* January 15, 1997.

S1089-5647(96)02731-9 CCC: $14.00

disulfides was determined to be in excess of 95% as measured from high-resolution mass spectra.[11] (C10−11, $C_{21}H_{44}O_2S_2$: MW found 392.278 93, calculated 392.278 26. C11−12, $C_{23}H_{48}O_2S_2$: MW found 420.310 31, calculated 420.309 57.)

11-Hydroxyundecyl 11′-Hydroxyundecyl 1,1′-Disulfide (C11−11) and 12-Hydroxydodecyl 12′-Hydroxydodecyl 1,1′-Disulfide (C12−12). $HO(CH_2)_nBr$ (n = 11, 12) was purified by column chromatography (silica, ethyl acetate:chloroform; 15:85, w/w) and converted to the corresponding thiols as described above. The ethanol solution of $HO(CH_2)_nSH$ (n = 11, 12) was titrated with I_2 in ethanol to form the symmetric disulfides. The $HO(CH_2)_nSS(CH_2)_nOH$ (n = 11, 12) was purified by column chromatography (silica, ethyl acetate:chloroform; 15:85, w/w). (C11−11, $C_{22}H_{46}O_2S_2$: MW found 406.293 72, calculated 406.293 91. C12−12, $C_{24}H_{50}O_2S_2$: MW found 434.323 76, calculated 434.325 23.)

Horse heart cytochrome *c* was purchased from Sigma. All other chemicals were purchased from Aldrich.

Electrode Fabrication. Au electrodes were fabricated by radio frequency sputtering *ca.* 3000 Å from a 99.99% Au target onto microscope slides through a special mask. A *ca.* 500 Å chromium layer was sputtered first to promote adhesion of the gold films. The Au electrodes were cleaned through successive exposures to chromic acid and aqueous HF, rinsed with water, and immediately placed into ethanolic disulfide solutions as described previously.[8] The Au electrodes were kept overnight in the *ca.* 5 mM solution of the corresponding ω-hydroxyalkyl disulfides prior to their use in the electrochemical studies. The geometric area of the electrodes was 0.13 cm^2.

Electrochemical Measurements. All electrochemical measurements were made using a BAS-100A electrochemical analyzer (Bioanalytical Systems) in solutions which had been purged with N_2 and were held at 0 °C in a jacketed electrochemical cell. All kinetic parameters were extracted from cyclic voltammograms obtained at a scan rate 5.12 V/s in aqueous solutions. The voltammograms for ferricyanide were obtained in 0.25 M CF_3COONa and 3 mM of the redox probe, while those for cytochrome *c* were obtained in 1.0 M KCl, 2 mM pH 7.1 phosphate buffer, and *ca.* 1 mM of the cytochrome. All potentials were measured and are reported versus a saturated calomel electrode.

***Ab Initio* Calculations.** *Ab initio* computations were performed using GAMESS.[12] Using previous theoretical approaches,[5,13] we have calculated α,ω-diradical splitting energies for the neutral triplet diradical using an unrestricted Hartree−Fock SCF calculation. The geometries of all the *trans* alkanes were optimized at the 3-21G basis set level prior to the introduction of the Li atom radical reporter groups.[14] The Li atoms were positioned 4 Å away from the hydrocarbon along the symmetry axis.

3. Results and Discussion

***Ab Initio* Predictions.** The electronic coupling through *all-trans* hydrocarbon chains has been the focus of several recent theoretical studies.[13,15] Estimates of the efficiency of electronic coupling between donor/acceptor pairs separated by hydrocarbons of differing lengths can be obtained from *ab initio* calculations using several methods. We have focused on the Koopman's theorem (KT) approximation in which the neutral triplet diradical splitting energies for a pair of nonbonded Li radicals positioned along the axis of the hydrocarbon chain is calculated. In these unrestricted Hartree−Fock calculations, the energy differences of the two highest occupied and the two lowest unoccupied eigenstates are summed to give a relative measure of the energy splitting due to electronic coupling through the intervening hydrocarbon chain. The sign of the electronic coupling arises from the symmetry of the lowest energy occupied and unoccupied orbitals. For hydrocarbons containing even numbers of carbons, the antisymmetric combination of Li radical orbitals is lower in energy. This results, by definition, in a negative splitting energy.[1,16] For hydrocarbons containing odd numbers of carbons, the symmetric combination of Li radical orbitals is lower, resulting in a positive coupling. A qualitative explanation of the origin of this difference in the coupling between even and odd chain length hydrocarbons can be presented from the work of Curtiss *et al.* which identified that the most important coupling pathways for these hydrocarbons stem from the overlap of the C−C antibonding orbitals.[13b,15] As seen in Figure 1, the electronic coupling along these antibonding orbitals stabilizes the symmetric combination of Li radical orbitals for odd chain length hydrocarbons, while the antisymmetric combination of Li radical orbitals is stabilized for even chain length hydrocarbons.

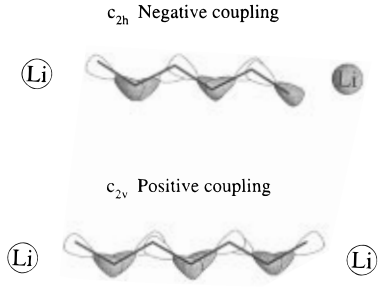

Figure 1. Drawing showing the origin of the sign alternation of the electronic coupling with the alkane spacer length. The interactions of the C−C antibonding orbitals for hexane and heptane spacers cause a change in the symmetry of the HOMO.

In the Fermi's golden rule limit appropriate for weakly coupled systems, the square of the splitting energy is proportional to the probability of electron tunneling through the hydrocarbon. Because the probability of electron tunneling for these nonadiabatic electron transfer reactions is directly proportional to the rate of electron transfer, the *ab initio* splitting energies can be used to predict electron transfer rates between donor/acceptor pairs as a function of the spacer geometry. The accuracy of these *ab initio* estimates has been demonstrated for hydrocarbon spacers *via* comparison to experimentally determined electronic coupling measurements.[5c,17] The Koopman's theorem splitting energies for nonbonded lithium radicals separated by a series of alkane spacers of increasing length yield an exponentially decreasing electron transfer rate with a decay constant, β, of 1.09 per methylene group,[18] in good agreement with the experimentally determined values.[3c,d,8a] The effect of subtle structural changes in ω-hydroxyalkanethiol monolayers on the electronic coupling has also been in good agreement with experiment.[4]

In order to probe quantum interference effects using this KT *ab initio* method, multiple hydrocarbon chains must be placed between the Li radical reporters. A requirement of the KT method is that the two radical reporter groups be in symmetry equivalent positions. Because the electronic-coupling-induced energy level splitting is small, even subtle asymmetry in the environment of the Li atoms can introduce energy splittings which overwhelm the electronic coupling component.[19] In order to probe the quantum interference between even and odd hydrocarbon chains lengths, one must consider donor/acceptor structures with symmetry equivalent Li sites. By surrounding a central C_{2h} symmetry hydrocarbon (even number of carbons) with two C_{2v} symmetry hydrocarbons (odd number of carbons) as shown in Figure 2, one can maintain the overall C_{2h} symmetry

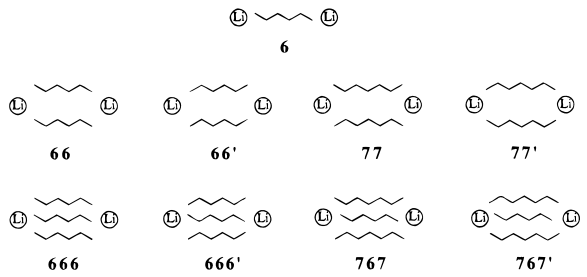

Figure 2. Schematic representation of the alkane spacer geometries used in the *ab initio* calculations. Beneath each structure is a representative numerical symbol.

TABLE 1: *Ab Initio* Dilithium Splitting Energies for Model Hydrocarbon Spacers

spacer designation[a]	ΔV^b ($\times 10^6$)	spacer designation[a]	ΔV^b ($\times 10^6$)
6	−128.1	77	4.9
66	−4.9	77′	14.2
66′	−4.9	767	−121.3
666	−131.6	767′	−112.1
666′	−131.9		

[a] The spacer designations are the same as in Figure 1. [b] Sum of anionic and cationic neutral triplet splitting energies in hartrees.

of the central hydrocarbon chain. We have considered all possible orientations of these hydrocarbons which display symmetry equivalent Li sites. The lithium radical splitting energies for these different spacers are collected in Table 1. The separation distance between the hydrocarbon chains of 4.75 Å was set to yield the same density of hydrocarbon chains found in the disulfide monolayers.[20]

The orientations of the hydrocarbon chains used in these *ab initio* calculations do not exactly mimic the structure of the monolayer on the Au surface.[6b,21] However, comparing the electronic coupling estimates for all these geometries leads to several useful generalizations. To a good approximation, the diradical splitting energies in the three hydrocarbon chain geometry are simply the sum of the splitting energies due to the central chain and the flanking chains. This additive property of the electronic coupling pathways is a likely result of weak interchain interactions. From the computational results in Table 1, a quantum interference effect between neighboring hydrocarbon chains is clearly observed. When the hexane chain is flanked by hexane chains, the Li orbital energy splitting increases. When heptane chains are used to flank the central hexane chain, the splitting energy decreases. This interference effect is independent of the orientations of the hydrocarbons in keeping with the qualitative explanation of the origin of this effect shown in Figure 1. The rotation of the hydrocarbon chains or the internal vibrational motion should not affect the sign of the electronic coupling contribution of each hydrocarbon chain.

The magnitude of this interference effect is small. The electronic coupling of the two Li radicals is mediated largely by the central hydrocarbon chain. The energy level splitting mediated by the two flanking hydrocarbons is approximately 1 order of magnitude weaker due to the larger separation between the terminal methyl groups and the Li radicals. The interference between these two pathways therefore yields a relatively small effect. The asymmetry in the tunneling pathways is essentially an artifact of the requirement to maintain the Li radicals in symmetry equivalent sites. From the additivity seen in the electronic coupling mediated through the chains, a stronger quantum interference effect would be anticipated when the Li atoms are positioned midway between the hexane and heptane chains.

The additivity of the electronic coupling pathways through each hydrocarbon chain allows a simple prediction of the size of the quantum interference effect. In a mixed monolayer containing randomly dispersed even and odd ω-hydroxyalkanethiolate chains, the electronic coupling is assumed to proceed equally through the shorter and longer chains. Because of the difference in the chain lengths, these two tunneling pathways will differ in their effectiveness at promoting electron transfer. The removal of a single methylene group within these hydroxyalkanethiol monolayers is observed to increase the rate of electron transfer by a factor of 2.9, which is equivalent to an increase in the electronic coupling splitting energy of $\sqrt{2.9}$ or 1.7.[8a] Relative to an electrode coated with only the longer ω-hydroxyalkanethiol monolayer, the electron transfer rate at the mixed monolayer-coated electrode would reflect each of the two pathways. Mathematically, one would sum the relative electronic coupling components for the shorter chains which occupy 50% of the sites, 0.5×1.7, and the longer chains which have the opposite sign, $0.5 \times (-1)$. This gives 0.35 which is squared to give 0.12 as the predicted electron transfer rate relative to the monolayer containing only the longer hydrocarbon chain length. The mixed monolayer would be 8 times more blocking as one composed of only the longer thiolate chains. If in contrast the electronic coupling added constructively, independent of the hydrocarbon chain length, this ratio would be $(0.5 \times (1.7 + 1))^2$ or 1.84.

Comparison with Experiment. We have measured the electron transfer rate for the reduction of ferricyanide and horse heart cytochrome *c* at electrodes coated with a range of symmetric and asymmetric ω-hydroxyalkane disulfides. These two redox probes were chosen because of the large difference in their radii. Figure 3 shows typical reduction rate curves for C10−11-, C11−11-, C11−12-, and C12−12-coated Au electrodes. The reduction currents measured at these electrodes have been corrected for diffusion and double-layer effects as described previously.[22] The reduction currents for the electrodes coated with the symmetric disulfide monolayers are in close agreement with previous measurements made using Au electrodes coated with ω-hydroxyalkanethiols of the same length.[18] From the simple quantum interference prediction, the currents for the C10−11- and C11−12-coated electrodes should be significantly lower than those coated with the C11−11 and C12−12, respectively. This is not observed. As seen in the experimental results collected in Table 2, we find that the electron transfer rates are quite consistent with the predictions which neglect the quantum interference effect.

There are several explanations for the absence of quantum interference in these measurements. The quantum interference observed in the *ab initio* calculations may be simply an artifact of the computational method and not relevant to the description of electronic coupling through these organic monolayers. For example, lateral coupling between adjacent hydrocarbon chains may invalidate the separation of the electronic coupling between individual hydrocarbon chains, which is at the heart of this quantum interference effect. An analogy to this false separation of tunneling pathways has been investigated by Liang and Newton for electron- and hole-tunneling pathways within individual hydrocarbon spacers.[5b] In this theoretical work, Liang and Newton found that for sufficiently long hydrocarbons the notion of separate electron-tunneling pathways which couple along unoccupied spacer orbitals and hole-tunneling pathways which couple along occupied orbitals was inappropriate due to the mixing between these pathways. Lateral electronic coupling between adjacent hydrocarbon chains within these densely packed monolayers may also mix the pathways involved in the

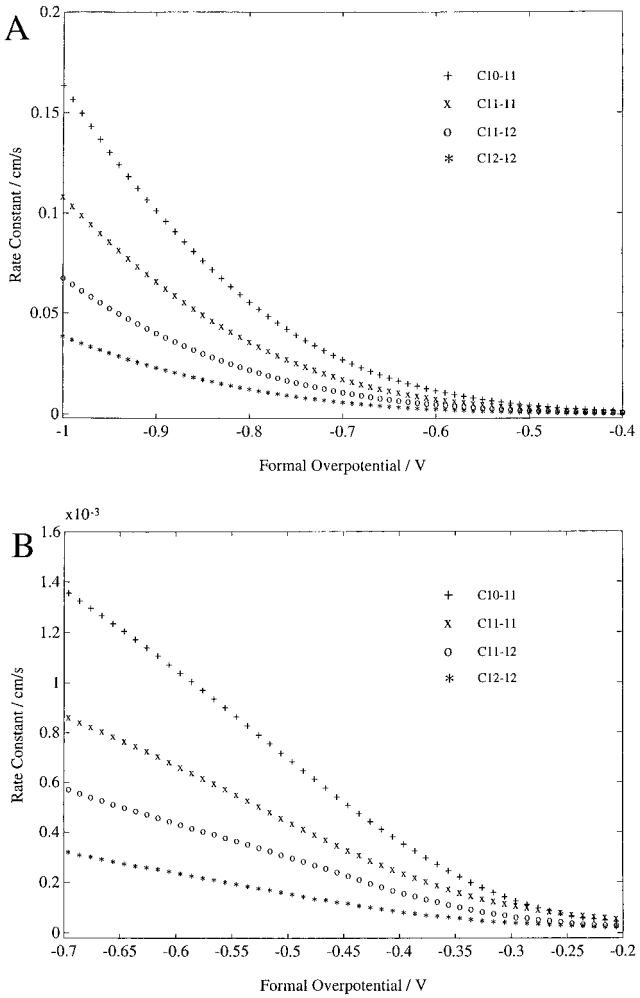

Figure 3. Heterogeneous electron transfer rate constants for Au electrodes derivatized with symmetric and asymmetric ω-hydroxyalkane disulfide monolayers as indicated in the legend. Figure 3A shows electron transfer rates for $Fe(CN)_6^{3-}$, while Figure 3B shows those measured for horse heart cytochrome *c*. These data were obtained from cyclic voltammograms and were corrected for diffusion and double-layer effects. Because these kinetic data give consistent reorganization values of 1.2 and 0.6 eV for the ferricyanide and cytochrome *c* redox probes, respectively, the relative electron transfer rates can be used as a direct measure of the electronic coupling differences between the monolayer-coated electrodes.

long-range electronic coupling. Such lateral coupling within alkanethiol monolayers has been recently reported by Slowinski *et al.*[23] Another complication is in the contact terms in the electronic coupling pathways between the exterior of the hydrocarbon chains and the redox molecule. The differing lengths of the ω-hydroxyalkanethiolate chains should introduce some surface corrugation within the asymmetric disulfide monolayers. Simplistically, the presence of a different thickness of solvent between the redox molecule and the thiolate chains may eliminate this interference effect. However, the presence of a different thickness of the solvent between the two thiolate chains would also be expected to lower the electronic coupling mediated through the shorter thiolate chain, giving rise to a more blocking mixed monolayer. That the ratios of the electron transfer rates for the asymmetric and the longer symmetric disulfide monolayer coated Au electrodes are close to those predicted for the absence of quantum interference argues against the presence of an increased solvent layer at the shorter thiolate chains.[24]

An alternate explanation for a lack of quantum interference for these mixed length thiolate chains focuses on the key

TABLE 2: Comparison of Relative Electron Transfer Rates between Experiment and Theoretical Predictions

monolayers	k_{ex}[a]	k_{nQI}[b]	k_{QI}[c]	k_{MCQI}[d] ($\beta' = 1.2$)	k_{MCQI}[d] ($\beta' = 2.0$)
		$Fe(CN)_6^{3-}$			
C10−11/C11−11	1.73 ± 0.23 (7)	1.84	0.12	0.35	0.57
C11−12/C12−12	2.02 ± 0.20 (6)	1.84	0.12	0.35	0.57
		Cytochrome *c*			
C10−11/C11−11	1.68 ± 0.14 (4)	1.84	0.12	0.28	0.39
C11−12/C12−12	1.75 ± 0.36 (4)	1.84	0.12	0.28	0.39

[a] k_{ex} is the experimentally determined electron transfer rate ratio for the indicated monolayer-coated electrodes. The numbers in parentheses correspond to the number of independent measurements used to determine the reported ratio. [b] k_{nQI} is the predicted electron transfer rate ratio in the absence of the quantum interference effect. [c] k_{QI} is the predicted electron transfer rate ratio in the presence of the quantum interference effect. [d] k_{MCQI} is the predicted electron transfer rate ratio in the presence of the quantum interference effect from the Monte Carlo model. The standard deviations for these determinations were <0.04 as determined from 10 separate runs.

assumption of the simple model. The electronic coupling through these asymmetric disulfide monolayers may not proceed evenly through both chains. Because of the very local nature of electronic coupling, each redox center will couple to the Au electrode through a relatively small number of alkyl chains. Even the small degree of phase segregation present within a random disulfide array could dramatically decrease the quantum interference effect.

Monte Carlo Predictions. In order to produce a more realistic quantum interference estimate, we have developed a Monte Carlo approach which probes the statistical nature of these electron transfer measurements. First we set up a 54×54 hexagonal grid onto which asymmetric disulfides are allowed "to react" and fill the grid. In each reaction cycle, a single grid site is selected at random along with one of the adjacent sites. If both are empty, the disulfide fills both sites. Otherwise, the adsorption fails and a new cycle is repeated. Typically 10 000 adsorption cycles are used. Following this adsorption cycle, the few remaining open sites are filled at random with either of the two thiolate chains. The electronic tunneling estimates are obtained by randomly allowing the redox probe to react with the grid. A point within the central 50×50 portion of the grid is selected at random, and the distances between the spherical redox probe and the 19 nearest neighbor ω-hydroxyalkanethiol chains are calculated. The tunneling estimate is calculated as the square of the mean of the square root of the terms for each thiolate chain (either -1 for the longer thiolate or 2.9 for the shorter thiolate multiplied by an exponential decay factor which takes into account each chain's distance from the redox probe.) The rates of a 1000 redox probes typically are averaged to obtain the estimated tunneling rate. The ratios of these Monte Carlo rates to those for the longer symmetric coated Au electrodes are given in Table 2.

There are two important input parameters within this model which affect the predicted quantum interference rate. The locality of the electronic coupling depends on both the exponential decay constant and the radius of the redox molecule. The decay constant appropriate for donors/acceptors separated in aqueous solutions has not been determined definitively. Using the Koopman's theorem *ab initio* approach for a pair of Li radicals separated by a row of water molecules of variable length, we have estimated this tunneling decay constant as 1.2 $Å^{-1}$.[18] The radius of the redox molecules was taken from crystallographic determinations.[25] For the smaller ferricyanide redox probe, this statistical model predicts a reduced quantum interference effect from that predicted if the electronic coupling

proceeds equally through the two chain lengths. By increasing the radius of the redox probe to that estimated for the heme redox center of cytochrome *c*, the quantum interference effect becomes larger within this model.[26]

The 1.2 $Å^{-1}$ estimate for the solution tunneling decay constant is likely too small due to the high symmetry of the row of water molecules used. In order to show the effect of this parameter on the predicted magnitude of the quantum interference effect, these calculations were repeated using an increased solution electron-tunneling decay constant. For both redox centers, as seen in Table 2, the quantum interference is observed to decrease when the solvent decay constant is increased to 2.0 $Å^{-1}$.[27]

Although the Monte Carlo model predicts a reduced quantum interference effect for randomly assembled asymmetric disulfide monolayers, the predicted ratios are still significantly lower than the experimental values, particularly for the larger cytochrome *c* redox probe. In order to eliminate the quantum interference effect within this model, the distribution of thiolate chains must be made distinctly nonrandom. However, the extent of phase segregation within these mixed thiolate monolayers would be expected to be quite small. In STM studies of asymmetric disulfides with hydroxyl and methyl terminal groups, Takami *et al.* were able to distinguish the different chains and found no measurable segregation of the chains.[7a] For the more subtly asymmetric disulfides used in the present work, the driving force for segregation would be expected to be much smaller.

In order to strengthen the assertion that phase segregation of the thiolate chains is not the reason for the absence of the quantum interference effect, the discussions above suggest several possible experimental improvements to probe for these interference effects. The effect of lateral segregation could be diminished by monitoring the electron transfer rate of a tethered redox probe assembled in diluent alkanethiolates of different lengths.[3a,c,e,f] At sufficient dilution, the covalently bound alkane chain pathway should sum with neighboring diluent chains, all with the same length. Alternately, one could tether the redox probe to the electrode surface *via* two covalent linkages of different lengths.

Acknowledgment. This work was supported by the National Science Foundation (CHE 9417357).

References and Notes

(1) Newton, M. D. *Chem. Rev.* **1991**, *91*, 767.

(2) Shephard, M. J.; Paddon-Row, M. N. *J. Phys. Chem.* **1995**, *99*, 17497.

(3) (a) Chidsey, C. E. D. *Science* **1991**, *251*, 919. (b) Miller, C.; Cuendet, P.; Grätzel, M. *J. Phys. Chem.* **1991**, *95*, 877. (c) Finklea, H. O.; Hanshew, D. D. *J. Am. Chem. Soc.* **1992**, *114*, 3173. (d) Xu, J.; Li, H.-L.; Zhang, Y. *J. Phys. Chem.* **1993**, *97*, 11497. (e) Weber, K.; Creager, S. E. *Anal. Chem.* **1994**, *66*, 3164. (f) Tender, L.; Carter, M. T.; Murray, R. W. *Anal. Chem.* **1994**, *66*, 3173.

(4) Cheng, J.; Saghi-Szabo, G.; Tossell, A. J.; Miller, C. J. *J. Am. Chem. Soc.* **1996**, *118*, 680.

(5) (a) Naleway, C. A.; Curtiss, L. A.; Miller, J. R. *J. Phys. Chem.* **1991**, *95*, 8434. (b) Liang, C.; Newton, M. D. *J. Phys. Chem.* **1992**, *96*, 2855. (c) Jordan, K. D.; Paddon-Row, M. N. *J. Phys. Chem.* **1992**, *96*, 1188.

(6) (a) Nuzzo, R. G.; Zegarski, B. R.; Dubois, L. H.; Allara, D. L. *J. Am. Chem. Soc.* **1987**, *109*, 733. (b) Nuzzo, R. G.; Flusco, F. A.; Allara, D. L. *J. Am. Chem. Soc.* **1987**, *109*, 2358. (c) Biebuyck, H. A.; Whitesides, G. M. *Langmuir* **1993**, *9*, 1766. (d) Biebuyck, H. A.; Bain, C. D.; Whitesides, G. M. *Langmuir* **1994**, *10*, 1825.

(7) (a) Takami, T.; Delamarche, E.; Michel, B.; Gerber, C.; Wolf, H.; Ringsdorf, H. *Langmuir* **1995**, *11*, 3876. (b) Bain, C. D.; Biebuyck, H. A.; Whitesides, G. M. *Langmuir* **1989**, *5*, 723. (c) Schönherr, H.; Ringdorf, H. *Langmuir* **1996**, *12*, 3891.

(8) (a) Becka, A. M.; Miller, C. J. *J. Phys. Chem.* **1992**, *96*, 2657. (b) Becka, A. M.; Miller, C. J. *J. Phys. Chem.* **1993**, *97*, 6233.

(9) The temperature and rate of addition of the I_2 reagent were both found to be important in completing the oxidation of the thiols. Excessive I_2 oxidizes thiols to form byproducts in the aqueous phase. Unreacted thiols in the oxidation reaction can be easily separated from the disulfide diols *via* column chromatography. Danehy, J. P.; Oester, M. Y. *J. Org. Chem.* **1967**, *32*, 1491.

(10) Hutchins, R. O.; Taffer, I. M. *J. Org. Chem.* **1983**, *48*, 1360.

(11) The purity was assessed by comparing the ratio of the asymmetric to symmetric disulfides from the MS spectrum. The asymmetric disulfides were found to undergo thiolate chains exchange to a small extent during the mass spectral analysis, making these purity figures a lower estimate to the true purity.

(12) Schmidt, M. W.; Baldridge, K. K.; Boatz, J. A.; Elbert, S. T.; Gordon, M. S.; Jensen, J. H.; Koseki, S.; Matsunaga, N.; Nguyen, K. A.; Su, S. J.; Windus, T. L.; Dupuis, M.; Montgomery, J. A. *J. Comput. Chem.* **1993**, *14*, 1347.

(13) (a) Liang, C.; Newton, M. D. *J. Phys. Chem.* **1993**, *97*, 3199. (b) Curtiss, L. A.; Naleway, C. A.; Miller, J. R. *J. Phys. Chem.* **1993**, *97*, 4050.

(14) (a) Binkley, J. S.; Pople, J. A.; Hehre, W. J. *J. Am. Chem. Soc.* **1980**, *102*, 939. (b) Gordon, M. S.; Binkley, J. S.; Pople, J. A.; Pietro, W. J.; Hehre, W. J. *J. Am. Chem. Soc.* **1982**, *104*, 2797. (c) Pietro, W. J.; Francl, M. M.; Hehre, W. J.; Defrees, D. J.; Pople, J. A.; Binkley, J. S. *J. Am. Chem. Soc.* **1982**, *104*, 5039.

(15) Curtiss, L. A.; Naleway, C. A.; Miller, J. R. *Chem. Phys.* **1993**, *176*, 387.

(16) Paddon-Row, M. N. *Acc. Chem. Res.* **1982**, *15*, 245.

(17) (a) Curtiss, L. A.; Naleway, C. A.; Miller, J. R. *J. Phys. Chem.* **1995**, *99*, 1182. (b) Beratan, D. N.; Hopfield, J.J. *J. Am. Chem. Soc.* **1984**, *106*, 1584.

(18) Cheng, J.; Miller, C. J. Unpublished data.

(19) Our attempts at isolating the electronic-coupling-induced splitting for even subtly asymmetric Li radicals have been unsuccessful. The asymmetry-induced splitting is typically several orders of magnitude larger than that due to the electronic coupling. Calculating the asymmetry-induced splitting by separately calculating the energy levels of a single Li atom on each side of the hydrocarbon chains is not sufficiently accurate to allow extraction of the electronic-coupling-induced splitting for these asymmetric systems.

(20) The separation distance between the hydrocarbon chains was calculated for hexagonal packing assuming that each chain occupies 19.5 $Å^2$.

(21) Ulman, A.; Eilers, J. E.; Tillman, N. *Langmuir* **1989**, *5*, 1147.

(22) Terrettaz, S.; Becka, A. M.; Traub, M. J.; Fettinger, J. C.; Miller, C. J. *J. Phys. Chem.* **1995**, *99*, 11216. The charge of horse heart cytochrome c was chosen to be +2 for the double-layer correction.

(23) Slowinski, K.; Chamberlain, R. V., II; Bilewicz, R.; Majda, M. *J. Am. Chem. Soc.* **1996**, *118*, 4709.

(24) We have produced asymmetric ω-hydroxyalkanethiol-containing chains differing in length by two methylene groups. The electron transfer ratios for these monolayers are significantly lower than those predicted, suggesting the presence of an extra layer of water between the shorter thiolate chain and redox molecule.

(25) (a) Bushnell, G.; Louie, G. V.; Brayer, G. D. *J. Mol. Biol.* **1990**, *214*, 585. (b) Vannerberg, N.-G. *Acta Chem. Scand.* **1972**, *26*, 2863.

(26) The effective radius for the cytochrome, 8.1 Å, was taken to be the distance from the iron to the solution edge of the heme proprionate.

(27) The 2.0 $Å^{-1}$ was chosen as an upper limit for the solvent tunneling decay constant. Its value was selected to be somewhat lower than that of the vacuum tunneling decay constant. Koopman's theorem *ab initio* calculations yield a vacuum tunneling decay constant of 2.3 $Å^{-1.18}$.